J. Fluid Mech. (1977), *vol.* 81, *part* 4, *pp.* 609–624
Printed in Great Britain

An analytical solution for the profile and volume of a small drop or bubble symmetrical about a vertical axis

By A. K. CHESTERS

Laboratory for Aero- and Hydrodyanmics,
Delft University of Technology, The Netherlands

(Received 21 September 1976)

A solution for the profile of a small drop or bubble symmetrical about a vertical axis and at rest in a second fluid is obtained as a first-order perturbation of a circle. At the end of the drop opposite the apex, the perturbation approach breaks down and a matching zero-gravity solution is used. The results agree with numerical solutions and indicate that the pendant-drop profile of maximum volume fitting a given small vertical tube intersects the exit plane at very nearly 90°. This enables the maximum volume to be determined accurately from a force balance.

1. Introduction

Numerical solutions for the equilibrium shape of a drop of fluid symmetrical about a vertical axis and at rest in a second (immiscible) fluid were obtained as early as 1883 by Bashforth & Adams and the number and accuracy of such solutions has since increased, the most recent contribution being the extensive tables of Hartland & Hartley (1976).

The case of a pendant drop or bubble attached to a vertical sharp-edged tube (figure 1) is of particular practical interest. The numerical results indicate that there exists a family of possible drop profiles one of which encloses a maximum volume $V_{\max}$. Experimentally, the slow growth of a pendant drop proceeds through a range of profiles until a critical volume V_{crit} is reached when part of the drop detaches itself. Whether $V_{\mathrm{crit}} = V_{\max}$ depends on whether all the equilibrium profiles reached during the growth process are stable to small perturbations. This has recently been shown to be the case for drops of constant volume on tubes of radius less than $3{\cdot}219(\sigma/\rho g)^{\frac{1}{2}}$, where σ represents the interfacial tension, ρ the difference in the densities of the fluids and g the acceleration due to gravity (Pitts 1976; Michael & Williams 1976).

The contribution of the present work is to provide an analytical solution for the profiles of small drops (or bubbles). A simple expression for $V_{\max}$ is also obtained. The analysis is first carried out for the case of a pendant drop or bubble and then extended (§ 5) to sessile drops or bubbles.

2. Profile of the lower part of a pendant drop

For simplicity the situation portrayed in figure 1 will be considered: here the drop density ρ_1 is greater than the density ρ_2 of the surrounding fluid, though the results obtained are equally applicable to the inverted situation (figure 2) in which $\rho_1 < \rho_2$,

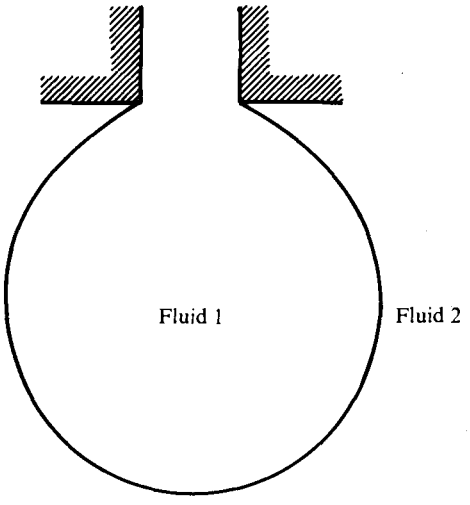

FIGURE 1

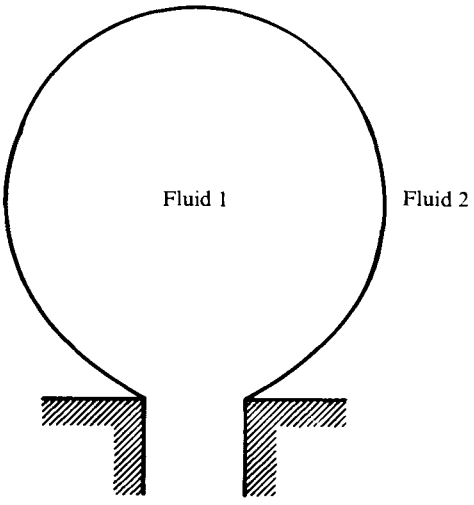

FIGURE 2

FIGURE 1. Pendant drop: $\rho_1 > \rho_2$.

FIGURE 2. 'Pendant' drop or bubble: $\rho_1 < \rho_2$.

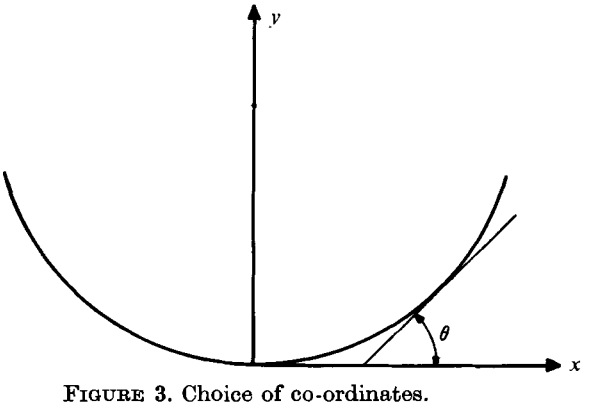

FIGURE 3. Choice of co-ordinates.

which includes the case of a 'pendant' bubble. The origin of the upward-pointing y axis and the horizontal x axis is taken as the apex of the drop (figure 3).

The equation of the drop profile is well known but will be derived for completeness. Assuming any flow into or out of the drop to be so slow that associated pressure variations and viscous stresses are negligible, the pressure variation in the two fluids is simply that required to balance gravitational forces:

$$p_1 = -\rho_1 gy + \text{constant}, \quad p_2 = -\rho_2 gy + \text{constant} \qquad (1), (2)$$

(p = pressure, g = acceleration due to gravity). The interface condition is that

$$p_1 - p_2 = \sigma(R_a^{-1} + R_b^{-1}) \qquad (3)$$

(σ = interfacial tension, R_a and R_b are respectively the radii of curvature of the interface in a plane containing the normal and the drop axis and in the perpendicular plane containing the normal, the radius being positive if the relevant centre of curvature lies on the drop side of the interface).

Elimination of p_1 and p_2 from (1)–(3), together with the requirement that $R_a = R_b = R$ (radius of curvature of the apex) at $y = 0$, yields

$$\sigma\left(\frac{1}{R_a}+\frac{1}{R_b}\right) = \frac{2\sigma}{R}-\rho g y, \tag{4}$$

in which $\rho = \rho_1 - \rho_2$. Substituting the appropriate expressions for R_a and R_b now yields the ordinary differential equation for the drop profile:

$$\frac{d^2y/dx^2}{[1+(dy/dx)^2]^{\frac{3}{2}}}+\frac{x^{-1}dy/dx}{[1+(dy/dx)^2]^{\frac{1}{2}}} = \frac{2}{R}-\frac{\rho g y}{\sigma}. \tag{5}$$

In dimensionless variables (5) becomes

$$\frac{d^2y'/dx'^2}{[1+(dy'/dx')^2]^{\frac{3}{2}}}+\frac{x'^{-1}dy'/dx'}{[1+(dy'/dx')^2]^{\frac{1}{2}}} = 2-\beta y', \tag{6}$$

in which $x' = x/R$, $y' = y/R$ and $\beta = \rho g R^2/\sigma$. The shape of the profile is thus evidently determined solely by the dimensionless parameter β (the 'shape factor'), while the scale is determined by R. Henceforth the primes will be dropped for simplicity.

An exact solution of (6) does not appear to exist, except for the special case $\beta = 0$ (zero gravity or $\rho_1 = \rho_2$), when a circle is obtained, corresponding to a spherical drop:

$$y = 1-(1-x^2)^{\frac{1}{2}}. \tag{7}$$

For small values of β the solution may be expected to resemble (7) closely over a large part of the drop profile and the obvious approach is therefore to apply perturbation methods. Before doing so, (6) will be written in the simpler form

$$\frac{1}{x}\frac{d}{dx}(x\sin\theta) = 2-\beta y, \tag{8}$$

in which

$$\tan\theta = dy/dx \tag{9}$$

(the primes now being omitted). Integration of (8) for the case $\beta = 0$ provides the differential form of (7):

$$x = \sin\theta. \tag{10}$$

For small β values the solution may be expected to have the form

$$x = (1+\epsilon)\sin\theta, \tag{11}$$

in which ϵ is a small quantity. Substitution of (11) in (8), neglecting products of ϵ and $d\epsilon/dx$, yields

$$x\,d\epsilon/dx + 2\epsilon = \beta y. \tag{12}$$

y may likewise be expected to lie close to the value given by (7):

$$y = [1-(1-x^2)^{\frac{1}{2}}](1-\eta), \tag{13}$$

in which η is a small quantity. Substitution of (13) in (12), neglecting products of β and η, yields

$$x\,d\epsilon/dx + 2\epsilon = \beta[1-(1-x^2)^{\frac{1}{2}}]. \tag{14}$$

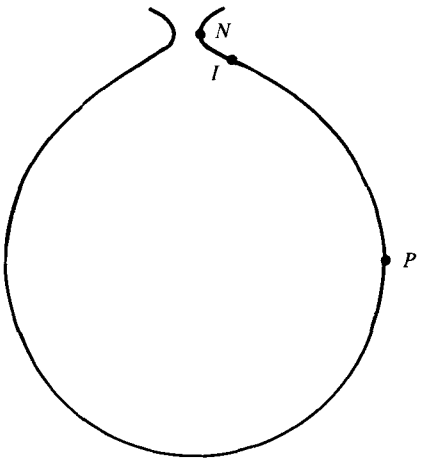

FIGURE 4

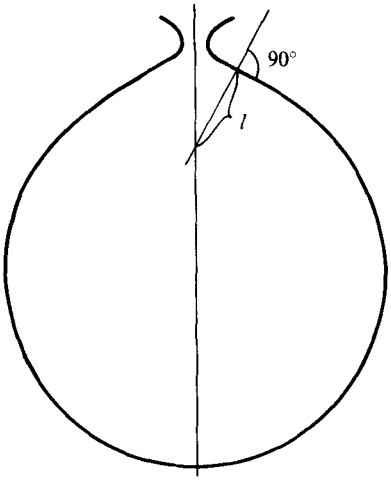

FIGURE 5

FIGURE 4. Profile of a pendant drop or bubble.

FIGURE 5. Magnitude of radius of curvature R_b.

At the drop apex $\epsilon = 0$,† and integration of (14), together with this condition, yields the following equation for the dependence of the perturbation parameter ϵ on β and x:

$$\epsilon = \beta\{\tfrac{1}{2} - [1-(1-x^2)^{\frac{3}{2}}]/3x^2\}, \tag{17}$$

the positive root applying in the vicinity of the apex.

Equation (17) indicates that ϵ increases from zero at the apex to a maximum of $\frac{1}{6}\beta$ at the point P (figure 4), at which $\theta = 0$ and $x \simeq 1$. Thereafter [with x decreasing and the negative root now required in (17)] ϵ decreases through zero towards large negative values as x becomes very small. At these small x values the expression for ϵ becomes

$$\epsilon = \beta[-2/3x^2 + 1 + O(x^2)] \tag{18}$$

and ϵ ceases to be 'small' at sufficiently small x values, whatever the value of β.

The perturbation approach thus breaks down at the top of the profile, indicating that the profile no longer resembles a circle there. The reason for this is that for non-zero values of β the profile does not close but forms a neck, afterwards widening again (figure 4). Qualitatively this can be explained as follows. The effect of the gravity term is to reduce the curvature of the profile, so that when it finally re-approaches the axis it does so at a shallower angle than in the circular, zero-gravity case. The radius of curvature R_b, which is in fact the length l in figure 5, therefore decreases rapidly, unlike the circular case, where it remains constant and equal to R. Since the sum $R_a^{-1} + R_b^{-1}$ is only a slowly varying function of y [equation (4)], the rapid increase in

† At the drop apex $\theta = x = 0$ and the dimensionless radius of curvature is 1. Hence

$$\frac{d^2y}{dx^2} = 1 = \frac{d}{dx}(\tan\theta) = \sec^2\theta\frac{d\theta}{dx} = \frac{d\theta}{dx}. \tag{15}$$

Differentiating (11), neglecting products of ϵ and $d\epsilon/dx$, gives $\cos\theta\, d\theta/dx = 1 - \epsilon - x\, d\epsilon/dx$, whence, at the apex,

$$d\theta/dx = 1 - \epsilon. \tag{16}$$

Combining (15) and (16) yields $\epsilon = 0$.

R_b^{-1} necessitates a decrease in R_a^{-1} to large negative values and the curve turns sharply away from the axis.

A solution for the neck region is developed in the next section. The rest of the present section is devoted to the integration of (11), using the expression obtained for ϵ, to obtain the profile of the lower part of the drop.

By combining (9) and (11), the differential equation of the (lower) drop profile is obtained:

$$\frac{dy}{dx} = \tan\theta = \frac{\sin\theta}{(1-\sin^2\theta)^{\frac{1}{2}}} = \frac{x}{[(1+\epsilon)^2-x^2]^{\frac{1}{2}}} \simeq \frac{x}{[1+2\epsilon-x^2]^{\frac{1}{2}}}, \tag{19}$$

since ϵ^2 is always negligible in comparison with ϵ. Except very close to P (figure 4), where x approaches 1,

$$2\epsilon/(1-x^2) \ll 1 \tag{20}$$

and an expansion of the root in (19), neglecting products of $2\epsilon/(1-x^2)$, gives

$$\frac{dy}{dx} = \frac{x}{(1-x^2)^{\frac{1}{2}}}\left(1-\frac{\epsilon}{1-x^2}\right). \tag{21}$$

Again, the positive root applies below the point P (figure 4).

On substituting from (13) for y, (21) gives

$$\frac{d}{dx}\{\eta[1-(1-x^2)^{\frac{1}{2}}]\} = \frac{\epsilon x}{(1-x^2)^{\frac{3}{2}}}$$

and on making use of the expression (17) for ϵ, this integrates to

$$\eta[1-(1-x^2)^{\frac{1}{2}}] = \tfrac{1}{6}\beta\{2\ln[1+(1-x^2)^{\frac{1}{2}}]+(1-x^2)^{-\frac{1}{2}}\}+\text{constant}.$$

At the apex, $x = 0$ and $(1-x^2)^{\frac{1}{2}} = 1$, yielding

$$\text{constant} = -\tfrac{1}{6}\beta[2\ln 2+1]$$

and

$$\eta[1-(1-x^2)^{\frac{1}{2}}] = \tfrac{1}{6}\beta\{2\ln\tfrac{1}{2}[1+(1-x^2)^{\frac{1}{2}}]+(1-x^2)^{-\frac{1}{2}}-1\},$$

i.e.

$$y = 1-(1-x^2)^{\frac{1}{2}}-\tfrac{1}{6}\beta\{2\ln\tfrac{1}{2}[1+(1-x^2)^{\frac{1}{2}}]+(1-x^2)^{-\frac{1}{2}}-1\}. \tag{22}$$

As mentioned above, (22) ceases to be valid as $x \to 1$, since the approximation (20) breaks down. In this region however, ϵ may be approximated by its maximum value

$$\epsilon = \tfrac{1}{6}\beta \tag{23}$$

and (19) reduces to

$$dy/dx = x/(1-x^2+\tfrac{1}{3}\beta)^{\frac{1}{2}}, \tag{24}$$

which integrates to

$$y = -(1-x^2+\tfrac{1}{3}\beta)^{\frac{1}{2}}+\text{constant}. \tag{25}$$

The constant is determined by the condition that the solutions (25) and (22) match in the zone where both are valid. This zone will exist only for sufficiently small β, the condition for the validity of (22) being (20) and that for the validity of (23) [and hence (25)] being obtained from an expansion of ϵ in the small quantity $1-x^2$:

$$\epsilon = \tfrac{1}{6}\beta[1-2(1-x^2)+O(1-x^2)^2],$$

which yields

$$1-x^2 \ll \tfrac{1}{2}.$$

If this condition is combined with (20) (in which ϵ is approximated by $\frac{1}{6}\beta$), an overlap zone is seen to exist for sufficiently small β, in which

$$\tfrac{1}{3}\beta \ll 1-x^2 \ll \tfrac{1}{2}. \tag{26}$$

In this zone (22) reduces to

$$y = -(1-x^2)^{\frac{1}{2}} - \tfrac{1}{6}\beta(1-x^2)^{-\frac{1}{2}} + [1+\tfrac{1}{6}\beta(1+2\ln 2)] + \text{smaller-order terms}$$

and (25) reduces to

$$y = \text{constant} - (1-x^2)^{\frac{1}{2}} - \tfrac{1}{6}\beta(1-x^2)^{-\frac{1}{2}} + \text{smaller-order terms},$$

whence

$$\text{constant} = 1+\tfrac{1}{6}\beta(1+2\ln 2)$$

and (25) becomes

$$y = -(1-x^2+\tfrac{1}{3}\beta)^{\frac{1}{2}} + 1 + \tfrac{1}{6}\beta(1+2\ln 2). \tag{27}$$

Equation (24) indicates that at the point P, where x is a maximum (figure 4),

$$1-x^2+\tfrac{1}{3}\beta = 0,$$

i.e.

$$x_P = 1+\tfrac{1}{6}\beta, \tag{28}$$

and from (27)

$$y_P = 1+\tfrac{1}{6}\beta(1+2\ln 2). \tag{29}$$

Sufficiently far above P, (22) again applies though not necessarily with the same constant of integration. The same matching procedure as applied above, however, indicates that the constant of integration *is* the same, so that (22) applies over the whole profile apart from the immediate vicinity of P, where (27) has to be used, and the upper part of the profile where the neck zone commences and ϵ is no longer small [equation (18)].

3. Profile of the neck of the drop

For small values of β the profile approaches very close to the axis before being deflected away to form the neck, and the height of the neck region is consequently small (of the order of β, as will be seen). The term on the right-hand side of (8) therefore varies very little over the neck zone and to the first approximation may be taken as constant, with a value corresponding to $y = 2$:

$$\frac{1}{x}\frac{d}{dx}(x\sin\theta) = 2(1-\beta) = \text{constant}. \tag{30}$$

Equation (30) is integrable and yields

$$x\sin\theta = x^2(1-\beta) + \text{constant}. \tag{31}$$

The constant is determined by the condition that the neck solution (31) and the perturbation solution (11) should match in the region adjoining the neck, although this will be the case only for sufficiently small β values. For such values the perturbation solution is valid down to small x values, ϵ being given by (18). Substitution for ϵ in (11) (neglecting products of ϵ) yields

$$x\sin\theta = x^2(1-\beta) + \tfrac{2}{3}\beta.$$

Comparison with (31) indicates that the constant is $\frac{2}{3}\beta$ and the neck solution becomes

$$\sin\theta = x(1-\beta) + \tfrac{2}{3}\beta/x. \tag{32}$$

Before integrating (32) to obtain the neck profile, the radius of the narrowest part of the neck (the point N in figure 4, where $\theta = 90°$) may be established. From (32),

$$1 = x_N(1-\beta) + 2\beta/3x_N,$$
$$x_N = \frac{1 \pm [1 - \frac{8}{3}\beta(1-\beta)]^{\frac{1}{2}}}{2(1-\beta)} = \tfrac{2}{3}\beta, \tag{33}$$

on choosing the appropriate sign and neglecting products of β. As will be seen, this value of x_N agrees with that arrived at by a simple force balance and thus provides a check on the preceding calculations.

The inflexion point I (figure 4) may also be located with the help of (32):

$$(d\theta/dx)_I = 0 = (1-\beta) - 2\beta/x_I^2,$$
$$x_I = [\tfrac{2}{3}\beta/(1-\beta)]^{\frac{1}{2}} = (\tfrac{2}{3}\beta)^{\frac{1}{2}} \tag{34}$$

to first order in β. Since this is the point at which the profile changes from concave to convex it may reasonably be said to be the boundary of the neck zone. Equation (18) indicates, however, that the perturbation solution is not yet applicable since

$$\epsilon = -1 + \beta = O(1).$$

Equation (32) may be integrated to obtain the neck profile as follows. After the substitutions

$$z = x(1-\beta), \quad \alpha = \tfrac{2}{3}\beta(1-\beta), \tag{35), (36}$$

(32) becomes

$$\sin\theta = (z^2 + \alpha)/z. \tag{37}$$

Substituting in (9) gives

$$dy/dx = \tan\theta = -(z^2+\alpha)/(z^2 - z^4 - 2\alpha z^2 - \alpha^2)^{\frac{1}{2}}, \tag{38}$$

where here and in subsequent expressions for the neck profile the positive root applies below the point N. Within the neck region $z \simeq x \ll 1$ and $\alpha \ll 1$ so the second and third terms within the root are always much smaller than the first and may be neglected. The fourth term, α^2, is of the same order as the first, z^2, close to N ($z_N = \alpha$) and so must be included:

$$\frac{dy}{dx} = (1-\beta)\frac{dy}{dz} = -\frac{z^2+\alpha}{(z^2-\alpha)^{\frac{1}{2}}}.$$

Integrating yields

$$y = \frac{1}{1-\beta}\left[-\frac{z(z^2-\alpha^2)^{\frac{1}{2}}}{2} + \left(\frac{\alpha^2}{4} + \frac{\alpha}{2}\right)\ln\left(\frac{z-(z^2-\alpha^2)^{\frac{1}{2}}}{z+(z^2-\alpha^2)^{\frac{1}{2}}}\right)\right] + \text{constant}. \tag{39}$$

Once again the constant may be established from the condition that the neck solution matches the perturbation solution. As noted above, at the point I the perturbation parameter ϵ is of order unity and according to (18) becomes 'small' only when

$$x^2 \gg x_I^2. \tag{40}$$

With the help of (34)–(36), (40) leads to the requirement in the matching zone that

$$z^2 \gg \alpha. \tag{41}$$

Making use of (41), together with (35) and (36), the neck profile (39) reduces to

$$y = -\tfrac{1}{2}x^2 - \tfrac{1}{3}\beta \ln (3x/\beta)^2 + \text{constant} + \text{smaller-order terms} \tag{42}$$

in the matching zone. Likewise the perturbation solution (22) reduces to

$$y = 2 - \tfrac{1}{2}x^2 + \tfrac{1}{3}\beta - \tfrac{1}{3}\beta \ln (\tfrac{1}{2}x)^2 + \text{smaller-order terms.} \tag{43}$$

Comparison of (42) and (43) indicates that the constant in (39) is equal to

$$2 + \tfrac{1}{3}\beta + \tfrac{1}{3}\beta \ln (6/\beta)^2,$$

and the neck profile is thus

$$y = \frac{1}{1-\beta}\left[-\frac{z(z^2-\alpha^2)^{\frac{1}{2}}}{2} + \left(\frac{\alpha^2}{4} + \frac{\alpha}{2}\right) \ln \left(\frac{z-(z^2-\alpha^2)^{\frac{1}{2}}}{z+(z^2-\alpha^2)^{\frac{1}{2}}}\right)\right] + 2 + \frac{\beta}{3}[1 + \ln (6/\beta)^2] \tag{44}$$

$$= \frac{-(1-\beta)x^2}{2}[1-(2\beta/3x)^2]^{\frac{1}{2}} + \frac{\beta}{3} \ln \left(\frac{1-[1-(2\beta/3x)^2]^{\frac{1}{2}}}{1+[1-(2\beta/3x)^2]^{\frac{1}{2}}}\right) + 2 + \frac{\beta}{3}[1 + \ln (6/\beta)^2] \tag{45}$$

to the first order in β.

The y co-ordinates of the points N and I can now be established. Substitution of (33) and (34) in (45) yields

$$y_N = 2 + \tfrac{1}{3}\beta[1 + \ln (6/\beta)^2], \tag{46}$$

$$y_I = 2 + \tfrac{1}{6}\beta \ln (6/\beta)^2 \tag{47}$$

to first order in β, and

$$y_N - y_I = \tfrac{1}{3}\beta[1 + \tfrac{1}{2} \ln (6/\beta)^2]. \tag{48}$$

The height of the neck zone, as characterized by $y_N - y_I$, is thus of the order of β, as mentioned earlier.

4. Volume enclosed by the profile

By a process of integration and matching similar to that used to establish the drop profile, the volume enclosed by the profile between the apex and horizontal plane may be calculated, the starting point being the formula

$$V = \pi \int x^2 dy = \pi \int x^2 \left(\frac{dy}{dx}\right) dx, \tag{49}$$

in which V is the dimensionless volume (= actual volume/R^3). The resulting expressions are:

$$V/\pi = \tfrac{1}{3}(1-x^2)^{\frac{1}{2}}(x^2+2) - \tfrac{1}{6}\beta(x^2 + (1-x^2)^{-\frac{1}{2}} + 3(1-x^2)^{\frac{1}{2}}) + \tfrac{2}{3}(1+\beta), \tag{50}$$

which, like (22), is valid everywhere except in the immediate vicinity of the point P and the neck of the drop;

$$V/\pi = \tfrac{1}{3}(1 - x^2 + \tfrac{1}{3}\beta)^{\frac{1}{2}}(x^2 + 2 + \tfrac{2}{3}\beta) + \tfrac{2}{3} + \tfrac{1}{2}\beta \tag{51}$$

for the immediate vicinity of P, the positive root applying in both (50) and (51) if the intersection with the horizontal plane is below the point P (figure 4);

$$V/\pi = x^2[1 - (\tfrac{2}{3}\beta/x)^2]^{\frac{1}{2}}(\tfrac{1}{4}x^2 + \tfrac{1}{3}\beta) + \tfrac{4}{3}(1+\beta) \tag{52}$$

for the neck region, the positive root applying if the intersection with the horizontal plane is below the point N (figure 4).

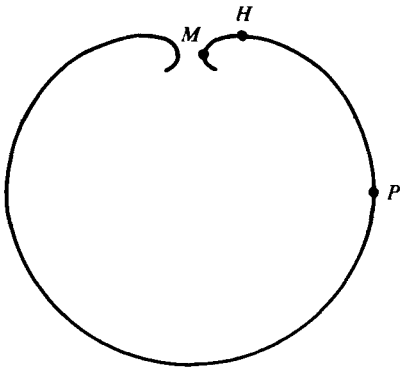

FIGURE 6. Profile of a sessile drop or bubble.

Special cases of the above formulae are the volumes enclosed by planes intersecting at the points P, I and N; these are obtained from the relevant x co-ordinates [(28), (34) and (33)]:

$$V_P/\pi = \tfrac{2}{3} + \tfrac{1}{2}\beta, \quad V_I/\pi = V_N/\pi = \tfrac{4}{3}(1+\beta). \tag{53)–(55}$$

To first order in β, V_I and V_N are equal since the first term of (52) makes a contribution of order β^2 in the region of the profile concerned.

5. Sessile drops

The general equations for the profile and volume of pendant drops derived above embody no assumptions as to the sign of β or the form of the surface and so are equally applicable to sessile† drops or bubbles for which β is negative ($\rho_1 < \rho_2$; see figure 6). The special equations for the values of x, y and V corresponding to the point P [(28), (29) and (53)] are likewise applicable.

No inflexion point I occurs in the profile of a sessile drop. Instead the extreme departure from a circular profile which occurs as the profile re-approaches the axis takes the form of a curling up of the profile on itself. The point H (figure 6) at which the profile becomes horizontal may be considered the analogue of the point I for a pendant drop, being the last point at which the profile remotely resembles a circle. From (32), the x co-ordinate of H is found to be the same as that of I for a pendant drop of equal $|\beta|$:

$$x_H = (-\tfrac{2}{3}\beta)^{\frac{1}{2}}. \tag{56}$$

The corresponding expressions for y_H and V_H are found from (45) and (52):

$$y_H = 2 + \tfrac{1}{3}\beta[2 + \ln(-6/\beta)], \quad V_H/\pi = \tfrac{4}{3}(1+\beta). \tag{57), (58}$$

The point M at which the profile again becomes vertical (figure 6) is analogous to the point N for a pendant drop. Putting $\theta = 270°$ in (32), M is found to have the same x co-ordinate as N in the case of a pendant drop of equal $|\beta|$:

$$x_M = (-\tfrac{2}{3}\beta)^{\frac{1}{2}}. \tag{59}$$

The corresponding expressions for y_M and V_M are found from (45) and (52) to be

$$y_M = 2 + \tfrac{1}{3}\beta[1 + \ln(6/\beta)^2], \quad V_M = \tfrac{4}{3}(1+\beta). \tag{60), (61}$$

† So termed for convenience, since they include the case of a drop of denser fluid 'sitting' on a horizontal surface.

	$\beta = 10^{-4}$	$\beta = 10^{-2}$	$\beta = 0{\cdot}03162$	$\beta = 0{\cdot}09550$
x_P	1·00002	1·00167	1·00527	1·01592
	1·00002	1·00168	1·00536	1·01668
x_I	$8{\cdot}16497 \times 10^{-3}$	$8{\cdot}16497 \times 10^{-2}$	0·145196	0·252322
	$8{\cdot}16578 \times 10^{-3}$	$8{\cdot}24789 \times 10^{-2}$	0·150007	0·280007
x_N	$6{\cdot}66667 \times 10^{-5}$	$6{\cdot}66667 \times 10^{-3}$	$2{\cdot}10819 \times 10^{-2}$	$6{\cdot}36662 \times 10^{-2}$
	$6{\cdot}66778 \times 10^{-5}$	$6{\cdot}77968 \times 10^{-3}$	$2{\cdot}22551 \times 10^{-2}$	$7{\cdot}57075 \times 10^{-2}$
y_P	1·00004	1·00398	1·01258	1·03798
	1·00004	1·00401	1·01291	1·04120
y_I	2·00037	2·02132	2·05529	2·13180
	2·00037	2·02160	2·05732	2·14385
y_N	2·00077	2·04598	2·12113	2·29544
	2·00077	2·04669	2·12691	2·33781
V_P	2·09455	2·11010	2·14407	2·24440
	2·09455	2·11025	2·14558	2·25918
V_I	4·18921	4·23068	4·32125	4·58882
	4·18921	4·23110	4·32557	4·63035
V_N	4·18921	4·23068	4·32125	4·58882
	4·18921	4·23121	4·32680	4·64601

TABLE 1. Pendant drops. The lower of each pair of values is the numerical result.

	$-\beta = 10^{-4}$	$-\beta = 10^{-2}$	$-\beta = 0{\cdot}03162$	$-\beta = 10^{-1}$
x_P	0·999983	0·998333	0·994730	0·983333
	0·999983	0·998342	0·994815	0·984151
x_H	$8{\cdot}16497 \times 10^{-3}$	$8{\cdot}16497 \times 10^{-2}$	0·145196	0·258199
	$8{\cdot}16415 \times 10^{-3}$	$8{\cdot}08481 \times 10^{-2}$	0·140846	0·236010
x_M	$6{\cdot}66667 \times 10^{-5}$	$6{\cdot}66667 \times 10^{-3}$	$2{\cdot}10819 \times 10^{-2}$	$6{\cdot}66667 \times 10^{-2}$
	—	—	—	—
y_P	0·999960	0·996023	0·987423	0·960228
	0·999960	0·996054	0·987730	0·963129
y_H	1·99957	1·97201	1·92362	1·79686
	1·99957	1·97239	1·92656	1·81742
y_M	1·99923	1·95402	1·87887	1·69371
	—	—	—	—
V_P	2·09424	2·07869	2·04472	1·93732
	2·09424	2·07883	2·04612	1·95049
V_H	4·18837	4·14690	4·05633	3·76991
	4·18837	4·14745	4·06162	3·78782
V_M	4·18837	4·14690	4·05633	3·76991
	—	—	—	—

TABLE 2. Sessile drops. The lower of each pair of values is the numerical result.

6. Comparison with numerical results

In tables 1 and 2 values of x, y and V at the characteristic points P, I and N (or P, H and M) calculated from the foregoing expressions are compared with the corresponding numerical results of Hartland & Hartley for values of $|\beta|$ up to about 0·1. The correspondence becomes closer the smaller $|\beta|$ is, the fractional difference in that

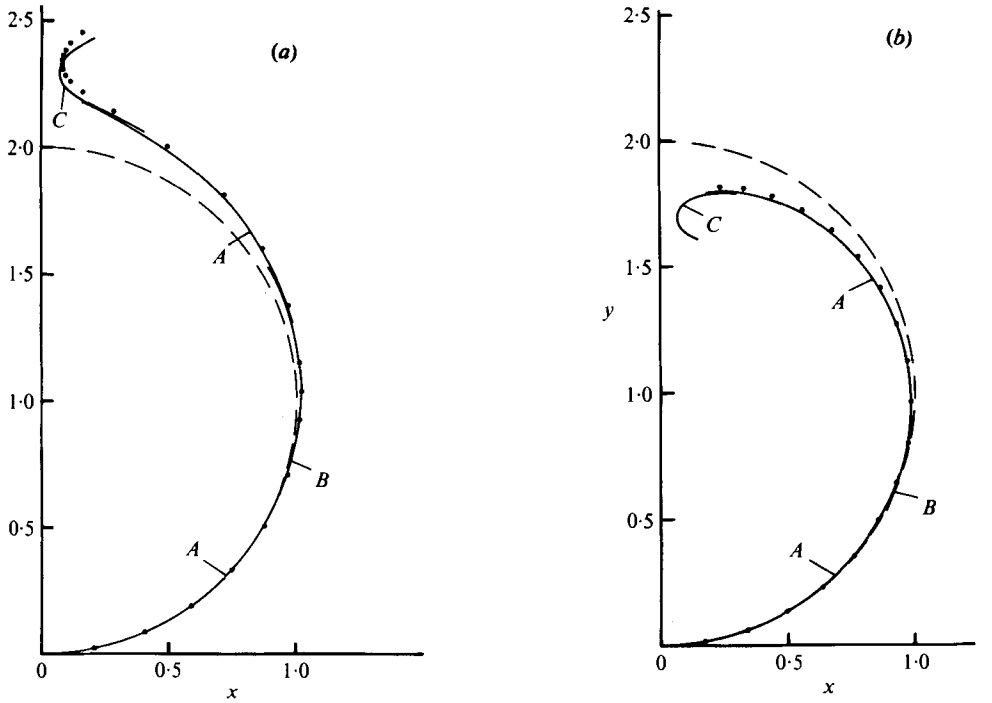

FIGURE 7. Profile of (*a*) a pendant drop ($\beta = 0{\cdot}0955$) and (*b*) a sessile drop ($\beta = 0{\cdot}1$). ●, numerical results (Hartland & Hartley); *A*, equation (22); *B*, equation (27); *C*, equation (45).

part of the quantity depending on β [for example in $V_P - \frac{4}{3}\pi$ in the case of V_P: see (53)] being of the order of β.

The full profiles for the larger two $|\beta|$ values are compared in figures 7(*a*) and (*b*).

7. Pendant drop profile of maximum volume

According to the wetting properties of the fluids concerned the circular bounding line between the two fluids and the material of the supporting tube may be either the inner or the outer edge of the tube mouth (figure 8). In either case the radius of this line will be called r and the angle at which the drop profile intersects the plane of the tube mouth ϕ. Unlike the contact angle between a fluid interface and a continuous solid plane, the angle ϕ is found experimentally to be capable of taking on a whole range of values,† and any intersection of a drop profile with a horizontal plane is therefore a possible junction between the drop concerned and a tube of appropriate radius.

During the growth of a pendant drop or bubble the plane of the tube mouth moves away from the apex of the profile (figure 9). The associated value of R, and hence the scale of the profile, first decreases, reaching a minimum when the drop is approximately hemispherical (figure 9, case *c*), and then increases until the plane of the tube mouth reaches the point N (case *e*). Further displacement of this plane (case *f*) necessitates

† The mechanism which enables equilibrium between the three media to occur at more than one ϕ value has not, to the author's knowledge, been elucidated. Is the boundary in fact located a very small distance from the solid edge, this microscopic distance varying with ϕ?

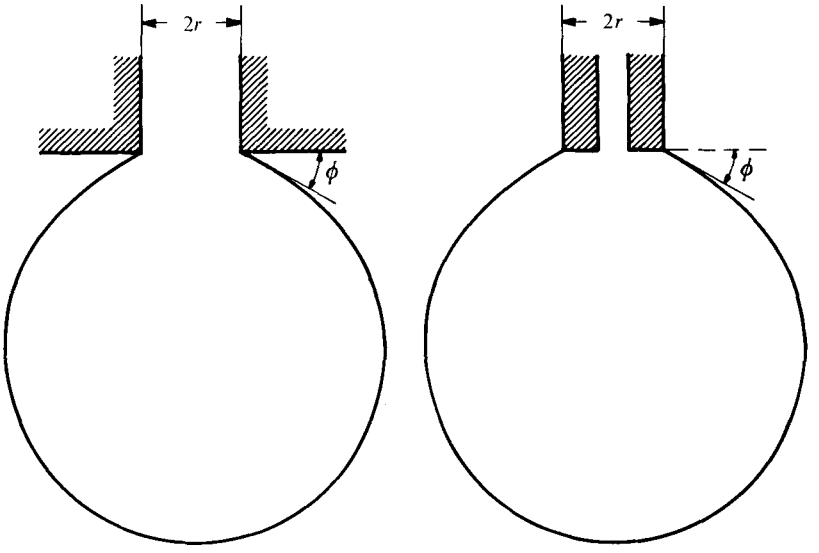

FIGURE 8. Pendant drop or bubble attached to a tube.

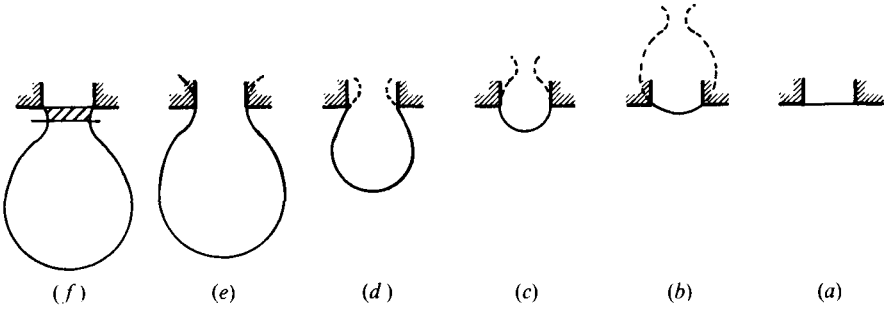

FIGURE 9. Growth of a pendant drop or bubble.

a decrease in the scale of the profile, and hence in the volume V_1 below the point N. Once the decrease in V_1 is no longer compensated by the increase in the volume V_2 enclosed above the point N (the shaded region) the maximum possible volume has been reached and further growth must result in detachment.

For small values of β, the point at which this occurs may be obtained from the previous results as follows. Reverting to the use of unprimed symbols to denote dimensional quantities, (33) gives

$$x_N/R = \tfrac{2}{3}\beta \tag{62}$$

to first order in β,

i.e.
$$x_N = \tfrac{2}{3}\rho g R^3/\sigma. \tag{63}$$

A reduction in x_N due to growth of the drop in stage (f) (figure 9) thus causes a reduction in R and so in β:

$$dx_N = \frac{2\rho g R^2}{\sigma} dR = 2\beta\, dR, \tag{64}$$

$$d\beta = \frac{2\rho g}{\sigma} R\, dR = 2\beta \frac{dR}{R}. \tag{65}$$

From (55), $$V_1 = \tfrac{4}{3}\pi R^3(1+\beta), \tag{66}$$

and use of (64) and (65) gives the corresponding reduction in V_1:

$$dV_1 = \tfrac{4}{3}\pi[3(1+\beta)R^2\,dR + R^3\,d\beta] = 4\pi R^2(1+\tfrac{5}{3}\beta)\,dR$$
$$= \frac{2\pi R^2}{\beta}(1+\tfrac{5}{3}\beta)\,dx_N \simeq \frac{2\pi R^2}{\beta}dx_N. \tag{67}$$

If the ratio of the tube radius r to x_N is written as

$$r/x_N = r/(\tfrac{2}{3}\beta) = 1+\tfrac{1}{2}\xi^2, \tag{68}$$

where ξ is expected to be very small, then (45) gives for the height δ of the shaded zone (figure 9, case *f*)

$$\delta = \tfrac{2}{3}\beta\xi R. \tag{69}$$

The volume V_2 of the shaded zone is thus

$$V_2 = \pi\overline{x^2}\delta \simeq \pi x_N^2\,\delta$$

since x varies between x_N and $x_N(1+\frac{1}{2}\xi^2)$ and ξ^2 is presumed very small. Thus

$$V_2 = \pi R^3(\tfrac{2}{3}\beta)^3\xi \tag{70}$$

and

$$dV_2 \simeq \pi R^3(\tfrac{2}{3}\beta)^3\,d\xi \tag{71}$$

since large fractional changes in ξ cause comparatively little variation in R and β.

The relation between $d\xi$ and dx_N may be found from (68):

$$x_N = r/(1+\tfrac{1}{2}\xi^2) \simeq r(1-\tfrac{1}{2}\xi^2), \tag{72}$$
$$dx_N = -r\xi\,d\xi \simeq -x_N\xi\,d\xi = -\tfrac{2}{3}\beta R\xi\,d\xi.$$

Use of (67), (71) and (72) shows that the criterion that the drop volume be a maximum is

$$dV_{\text{drop}} = 0 = dV_1 + dV_2$$
$$= -\tfrac{4}{3}\pi R^3\xi\,d\xi + \tfrac{8}{27}\pi R^3\beta^3\,d\xi,$$

i.e. $$\xi = \tfrac{9}{2}\beta^3. \tag{73}$$

The value of ξ is indeed extremely small and it is evident that the maximum-volume situation is very close to that in which the point N lies in the plane of the tube mouth (figure 9, case *e*), for which

$$x_N = r, \quad \delta = 0, \quad V_{\text{drop}} = V_N, \quad \phi = \tfrac{1}{2}\pi.$$

The corresponding values for the maximum-volume case are found from (73) to be

$$x_N = r(1-\tfrac{1}{2}\xi^2) = r(1-\tfrac{2}{81}\beta^6), \quad \delta/R = \tfrac{2}{3}\beta\xi = \tfrac{4}{27}\beta^4,$$
$$V_{\max} = (V_{\text{drop}})_{\phi=\frac{1}{2}\pi}(1+\tfrac{2}{81}\beta^6),$$
$$\phi = \tfrac{1}{2}\pi + \xi = \tfrac{1}{2}\pi + \tfrac{2}{81}\beta^3,$$

i.e. $$\sin\phi = 1-\tfrac{2}{81}\beta^6. \tag{74}$$

The differences between the two sets of values of x_N and V_{drop} are of a much smaller order than the accuracy of the expressions previously obtained for x_N and V_N, so these expressions apply with equal accuracy to the maximum-volume case:

$$V_{\max} = \tfrac{4}{3}\pi R^3(1+\beta), \quad x_N = r = \tfrac{2}{3}\beta R. \tag{75), (76}$$

Since β is a function of R, R may be eliminated from (75) and (76) to obtain $V_{\max}$ as a function of r. As (75) is accurate to only first order in β, the resulting expression cannot be stated more accurately than as

$$V_{\max} = 2\pi r\sigma/\rho g. \tag{77}$$

Equation (74) indicates that the amount by which $\sin\phi$ differs from 1 in the maximum-volume case is extremely small ($\sim 10^{-8}$ for $\beta = 0{\cdot}1$). The approximation

$$\sin\phi = 1 \tag{78}$$

must therefore remain valid up to β values considerably greater than those at which the other predictions of the present theory apply. This is made use of in the next section to obtain an expression for $V_{\max}$ of greater accuracy and wider applicability than (77).

8. Maximum volume derived from a force balance

The approximation (78) for the profile of maximum volume enables a simple force balance to be performed. The forces acting on the drop are as follows (figure 10).

(1) An upward surface-tension force of magnitude $2\pi r\sigma$.

(2) The weight of the drop: $V_{\max}\rho_1 g$.

(3) The downward force due to the pressure of the drop fluid in the plane of the tube mouth: $\pi r^2(p_1)_{\text{mouth}}$.

(4) The upward force due to the pressure of the external fluid on the outer surface of the drop.

Were the pressures inside and outside the drop equal in the mouth plane, the total pressure force would be the same as if the drop were wholly surrounded by fluid 2, namely the Archimedes upward buoyancy force $V_{\max}\rho_2 g$. The force balance then leads to (77), often called Tate's law. In general, however, $(p_1)_{\text{mouth}} \neq (p_2)_{\text{mouth}}$ and the sum of forces 3 and 4 is the upward force $V_{\max}\rho_2 g - \pi r^2(p_1 - p_2)_{\text{mouth}}$. The total force balance then gives

$$V_{\max}\rho_2 g - \pi r^2(p_1 - p_2)_{\text{mouth}} + 2\pi r\sigma - V_{\max}\rho_1 g = 0,$$

i.e.
$$V_{\max}\rho g = 2\pi r\sigma - \pi r^2(p_1 - p_2)_{\text{mouth}}. \tag{79}$$

The pressure difference in the plane of the tube mouth may, with the help of (1) and (2), be expressed in terms of the pressure difference $2\sigma/R$ at the apex and the height of the drop h (figure 10):

$$(p_1 - p_2)_{\text{mouth}} = 2\sigma/R - g\rho h. \tag{80}$$

Combining (79) and (80) gives

$$V_{\max}\rho g = 2\pi r\sigma - \pi r^2(2\sigma/R - g\rho h),$$

i.e.
$$V_{\max} = (2\pi r\sigma/\rho g)f, \tag{81}$$

where
$$f = 1 - \frac{r}{R}\left(1 - \beta\frac{h}{2R}\right). \tag{82}$$

The factor f represents the degree to which $V_{\max}$ differs from the value given by Tate's law. Since $r/R = O(\beta)$ and $h/2R = O(1)$ the two terms by which f departs from 1 are

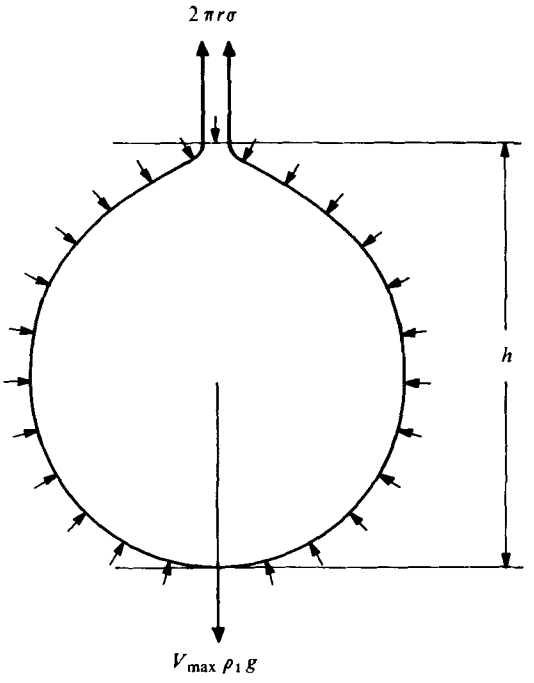

FIGURE 10. Force balance.

seen to be of the order of β and β^2. An accurate expression for these terms may be obtained as a function of the dimensionless quantity

$$\chi = r(3V_{\max}/4\pi)^{-\frac{1}{3}} \tag{83}$$

as follows.

From (75) and (46) (which applies since the point N lies, within the accuracy of (46), in the plane of the tube mouth),

$$1/R = (4\pi/3V_{\max})^{\frac{1}{3}}[1+\tfrac{1}{3}\beta+O(\beta^2)] \tag{84}$$

and

$$h/2R = 1+O(\beta). \tag{85}$$

Substituting (84) and (85) in (82) yields

$$\begin{aligned} f &= 1-\chi[1+\tfrac{1}{3}\beta+O(\beta^2)]\,[1-\beta+O(\beta^2)] \\ &= 1-\chi[1-\tfrac{2}{3}\beta+O(\beta^2)]. \end{aligned} \tag{86}$$

Furthermore, from (84) and (76),

$$r/R = \chi[1+\tfrac{1}{3}\beta+O(\beta^2)] = \tfrac{2}{3}\beta+O(\beta^2). \tag{87}$$

Hence $\chi = O(\beta)$ and (87) reduces to

$$\beta = \tfrac{3}{2}\chi+O(\chi^2). \tag{88}$$

Substituting (88) in (86) gives

$$f = 1-\chi+\chi^2+O(\chi^3). \tag{89}$$

The value of χ is not directly calculable from values of r, ρ, σ and g and it is therefore

more useful to obtain an expression for f in terms of the directly calculable dimensionless quantity β_0:†

$$\beta_0 = (\tfrac{2}{3}\rho g r^2/\sigma)^{\frac{1}{2}}. \tag{90}$$

The relation between β_0 and χ is obtained by substitution of (89) in (81):

$$\frac{V_{\max}}{\frac{4}{3}\pi r^3} = \frac{1}{\chi^3} = \frac{f}{\beta_0^3} = \frac{1-\chi+\chi^2+O(\chi^3)}{\beta_0^3}, \tag{91}$$

$$\chi = \beta_0[1+\tfrac{1}{3}\chi-\tfrac{1}{9}\chi^2+O(\chi^3)] = O(\beta_0). \tag{92}$$

Substituting this expression for χ into the right-hand side of (91) yields

$$\chi = \beta_0[1+\tfrac{1}{3}\beta_0+O(\beta_0^2)]. \tag{93}$$

Substitution of (93) in (89) gives f as a function of β_0:

$$f = 1-\beta_0+\tfrac{2}{3}\beta_0^2+O(\beta_0^3). \tag{94}$$

From this equation, together with (81), the value of $V_{\max}$ is directly calculable from r, ρ, σ and g.

The relation between β and β_0 is obtained from (88) and (93):

$$\beta = \tfrac{3}{2}\beta_0+O(\beta_0^2). \tag{95}$$

The restriction of the present analysis to values of β small in comparison with unity thus implies a similar restriction on β_0 and thereby on the size of the tubes concerned. The tube radius at which the pendant profiles become unstable to small perturbations, $3{\cdot}219(\sigma/\rho g)^{\frac{1}{2}}$, corresponds to a β_0 value of 1·9 and so lies far outside the range of tube sizes considered here.

REFERENCES

Bashforth, F. & Adams, H. 1883 *The Theories of Capillary Action*. Cambridge University Press.

Hartland, S. & Hartley, R. W. 1976 *Axisymmetric Fluid–Liquid Interfaces*. Elsevier.

Michael, D. H. & Williams, P. G. 1976 The equilibrium and stability of axisymmetric pendent drops. *Proc. Roy. Soc.* A **351**, 117–127.

Pitts, E. 1976 The stability of a drop hanging from a tube. *J. Inst. Math. Appl.* **17**, 387–397.

† The suggestion that f could be expressed as function of β_0 is due to Prof. J. R. A. Pearson.